Identifying the Thermal Parameters and Controlling the Temperature of a High-Altitude Balloon Payload

Douglas R. Isenberg[1], Brian M. Rookaird[2], Jacob Weisshaupt[3], Jessica Smith[4] , Bryan Winterling[5]

Embry-Riddle Aeronautical University, Prescott, AZ, 86301

This paper describes the lumped-parameter modeling, identification, and control of the payload temperature inside a high-altitude balloon gondola. Experimental methods for identifying the lumped thermal resistance and thermal capacitance at the launch-altitude and at high-altitude are described. Utilizing the identified values, both a pressure-independent model and a pressure-dependent model are formulated. With knowledge of the thermal resistance, a bang-off control system is sized to keep the payload temperature above a prescribed limit. Both of the closed-loop models are validated with recorded flight data.

I.   Introduction

MAINTAINING a payload temperature within the maximum and minimum rated component specifications is one of the challenges encountered in carrying out high-altitude experiments [1]. In order to achieve suitable thermal control, it is necessary to have some knowledge of the heat-transfer characteristics of the subsystems that comprise a gondola.

Modeling of the heat-transfer characteristics of high altitude balloon gondolas has been an area of study since the 1960's. The focus of much of the early research has been on long-duration flights where radiative heat-transfer dominates the thermal dynamics of a gondola. Design guidelines for passive thermal control that are intended mitigate the effects of solar radiation are proposed in [2] and include the use of a conductive gondola surface, a gondola surface coating with a high absorptivity and low emissivity, and the use of water as a means of heat storage. In [3], a scientific payload with an aluminum foil surface coating that sustained damage caused by high-temperatures is examined. Contradicting one of the recommendations in [2], it was determined through steady-state analysis that the low emissivity of the aluminum foil resulted in heat dissipation at an insufficient rate which lead to over-heating. A general thermal model is described in [4] and [5]. Here, the gondola is modeled as an isothermal

---

[1] Assistant Professor, Dept. of Aerospace and Mechanical Engineering, isenberd@erau.edu, AIAA Member
[2-5] Students, Dept. of Aerospace and Mechanical Engineering

sphere in order to simplify the radiation heat-transfer geometry. This methodology produced results that were in close agreement with the measured flight temperatures. More contemporary studies have been carried out with numerical software packages [6-7].

Short duration flights lasting only a few hours are becoming popular for both educational and scientific purposes. Since a float altitude is not sustained for a significant amount of time on these flights, the effects of radiative heat-transfer are de-emphasized while the effects of initial payload temperature and internal heat dissipation become more pronounced. In this paper, a system identification approach is utilized to develop a lumped-parameter thermal model for a high-altitude balloon gondola intended for short-duration flights. In order to accomplish this, three experiments are carried out as part of the identification process. Two of the experiments are utilized to find the equivalent thermal resistance and capacitance of the gondola at both the launch-altitude and at the burst-altitude. In one of the examined approaches, the parameters are treated as pressure-dependent, and a linear regression is utilized to quantify their pressure dependence. Another approach is considered in which the parameters are treated as constants. The third identification experiment is utilized to find the net heat-transfer due to radiation at the launch-altitude. Since the analytical calculation of the radiative heat-transfer would require several estimations concerning the emissivity and absorptivity of the gondola as well as many broad assumptions concerning the ever-changing geometry of the problem [8], it is currently assumed that the measured experimental value remains constant throughout the flight. Utilizing the identified model, a feedback bang-off temperature controller is designed and incorporated into the model. Lastly, the validity of both the pressure-dependent model and pressure-independent model of the gondola pictured in Fig. 1 are tested with actual flight-data.
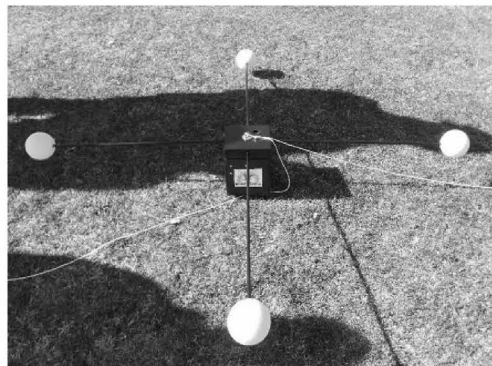
Fig. 1 Preflight gondola.

II. Heat Transfer Dynamics

Lumped-parameter thermal models are developed by decomposing a structure into a finite number of isothermal nodes and formulating a power balance for each node [9-10]. The power balance takes is of the form:

$$\begin{matrix} \textit{Rate of} \\ \textit{energy} \\ \textit{stored} \end{matrix} = \begin{matrix} \textit{Rate of} \\ \textit{energy} \\ \textit{gained} \end{matrix} - \begin{matrix} \textit{Rate of} \\ \textit{energy} \\ \textit{lost} \end{matrix} . \qquad (1)$$

While it is possible to decompose the entire gondola and its internal components into many thermal nodes, such an approach is not followed in this work. There are several reasons for this decision. From a practical standpoint, the system identification experiment would require an extensive amount of instrumentation. More importantly, high-order identification approaches tend to result in many characteristic modes, a number of which may not have much effect on the isothermal node that is really of interest, the scientific payload [11]. Furthermore, the nodes that give rise to the dominant modes are not a-priori knowledge. By selecting only one thermal node, the effects of the the non-dominant modes are treated as both perturbations and noise and a best-fit first-order lumped parameter model is easily obtained.

A graphical representation of the system is shown in Fig. 2. The gondola is a composite structure comprised of Nomex honeycomb carbon fiber paneling with an internal foam insulation lining. The payload consist of electronic circuit boards and cameras. The ability of the payload and gondola to store heat is lumped into the thermal capacitance parameter, C_P. The resistance to heat flow from outside the gondola to the payload as well as from the payload to outside of the gondola is lumped into the thermal resistance parameter, R_P. The power dissipated by the
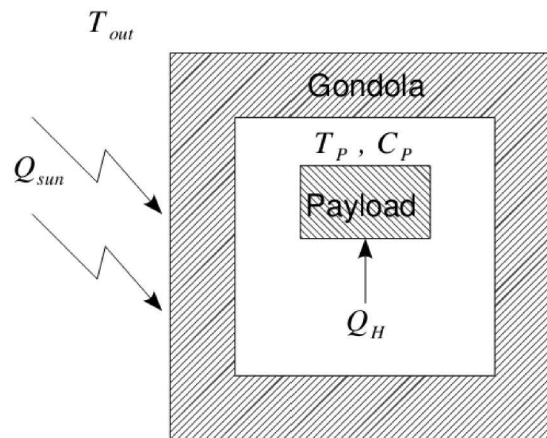
Fig. 2 Heat transfer model.

experiment electronics and cameras is considered to be negligible. However, a feedback controlled resistive heater provides the internal input heat, Q_H, to the payload. Furthermore, the gondola, and thus the payload, receives a significant amount of heat from direct solar, albedo, and planetary radiation, the effects of which are lumped into the term Q_{sun}. Applying the power balance described in (1), one obtains:

$$C_p \frac{dT_p}{dt} = -\frac{1}{R_p}(T_p - T_{out}) + Q_H + Q_{sun} .$$ (2)

The left-hand term in (2) is the rate of energy stored in the payload, and the last two terms on the right-hand side are direct sources of heat applied to the system. The first term on the right-hand side can be attributed to Newton's law of cooling in the case of convection but also describes one-dimensional conduction through a constant temperature gradient [10]. The term also approximates radiative heat-transfer, which can be shown by linearizing the Stefan-Boltzmann equation about the normal operating temperatures [9]. The actual method of heat transfer that is taking place will depend upon the altitude of the payload. Both convection and radiation are expected at the launch-altitude, while significantly more heat-transfer via radiation is expected at the balloon burst-altitude. Regardless, the heat that is lost to the atmosphere is not considered to significantly alter the outside atmospheric temperature, T_{out}.

III.   System Identification

The lumped parameter heat-transfer dynamics in (2) is described by a first-order ordinary differential equation. Assuming that experiments are devised such that T_{out} and $Q_H + Q_{sun}$ are kept constant, the solution of (2) has the form

$$T_P(t) = k_1 e^{\left(\frac{-t}{R_p C_p}\right)} + k_2$$

$$k_1 = T_P(0) - T_P(\infty)$$
$$k_2 = T_P(\infty)$$ (3)

When $t = R_P C_P$, then

$$T_P(R_P C_P) \approx 0.37 \left(T_P(0) - T_P(\infty)\right) - T_P(\infty) .$$ (4)

Given a sufficient amount of time such that the steady-state condition is reached, the right-hand side of (4) is easily computed from recorded data. The time-constant, $R_P C_P$, can then be obtained from a plot of the temperature

evolution.

For heat-transfer problems, the dynamics are often very slow, thus it may take an inconvenient amount of time to reach steady-state. An alternative approach is to fit the collected experimental data to an equation in the form of (3) using a nonlinear least-squares algorithm.

Assuming that either steady-state is obtained or that the collected data has been fit to a model in the form of (3), then the thermal resistance is found as

$$R_P = \frac{T_P(\infty) - T_{out}}{Q_H + Q_{sun}} , \qquad (5)$$

and then the thermal capacitance can be computed from the identified time-constant.

Assuming that the thermal resistance and thermal capacitance are dependent upon the atmospheric pressure, they can be considered to be a function of time as the gondola ascends and descends. With this view, (2) describes a time-varying linear system in which case the methodology described above is not valid. However, the time-constant method can be used to identify the thermal parameters at specific instances of pressure by keeping pressure constant throughout the experiment. The pressure dependence can then be approximated via a linear regression by utilizing the identified parameters at both a launch-altitude pressure and a high-altitude pressure.

- **Identification at Launch-Altitude Pressure**

The identification experiment at launch-altitude $\left(P = 100.3 \ (kPa) \right)$ was performed at room temperature with minimal forced-air convection and away from direct sunlight. Three $15 \ \Omega$ ceramic power resistors were placed inside the gondola and connected in parallel to a 5 V laboratory power supply which ideally delivers 5 W to the inside of the gondola when the supply is switched on, though the actual measured power was 4.86 W. Previous experiments have shown the thermal time-constant of the ceramic resistors to be relatively small which can be seen in the collected data, so their heat transfer dynamics are neglected from the model. A thermocouple, routed through the package, was used to measure the payload temperature, T_P, and a second thermocouple was utilized to measure the outside temperature, T_{out}.

The instrumented gondola was given a sufficient amount of time to reach the steady-state temperature at which point the 4.86 W heat source was switched on. The payload temperature was then measured on one minute intervals until the payload reached a near steady-state temperature. The recorded temperature of the payload vs. time is
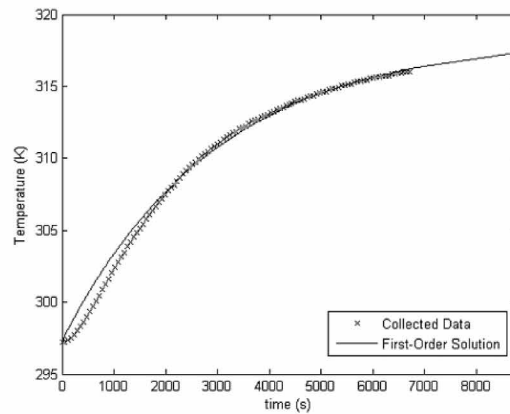
Fig. 3 Launch-altitude experiment.

plotted in Fig. 3.

A nonlinear least-squares curve fitting algorithm was utilized to fit an equation in the form of (3) to the collected data. The data points received weights that linearly increase with the time so that the low-frequency dynamics were captured more than the high-frequency dynamics that are initially dominant. Using this approach, the time-constant can be found to be approximately $R_P C_P = 2930.4$. Since the experiment was performed away from direct sunlight, it is assumed that the solar heating is zero, $Q_{sun} = 0 \ (W)$. Then, the only source of direct heat is $Q_H = 4.86 \ (W)$. Using the estimated steady-state temperature and the average outside temperature, $T_{out} = 295.03 \ (K)$, the thermal resistance is obtained as $R_P = 4.8025 \ (K/W)$ which means the thermal capacitance must be $C_P = 610.18 \ (J/K)$. A plot of the identified first-order system response is included in Fig. 3.

- **Identification at High-Altitude Pressure**

The high-altitude identification experiment was performed inside a vacuum chamber at an atmospheric pressure that varied between 1033.3 Pa and 959.9 Pa. which corresponds to an altitude well over 30 km. Three 15 Ω resistors were once again placed inside the gondola and connected to a nominal 5 V source which dissipated a measured 4.34 W. Again, a thermocouple was utilized to measure the payload temperature. An additional thermocouple was utilized to measure the chamber wall temperature which remained at a fairly constant 292.6 K. The vacuum chamber was allowed to reach steady-state pressure and then the heaters were turned on. The payload temperature was then measured every minute. The recorded temperature is depicted in Fig. 4.

A nonlinear least-squares algorithm was again used to fit a curve in the form of (3) to the collected data from
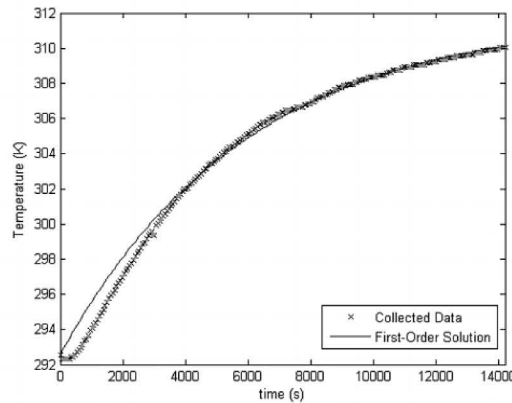
Fig. 4 High-altitude experiment.

which the time-constant was found to be $R_P C_P = 5891.0$. Utilizing $T_{out} = 292.6 \ (K)$ and assuming that $Q_{sun} = 0 \ (W)$ such that the total applied heat was $Q_H = 4.34 \ (W)$, the thermal resistance is $R_P = 4.3924 \ (K/W)$ which implies that the thermal capacitance is $C_P = 1341.2 \ (J/K)$. The response of the identified linear system is also depicted in Fig. 4.

- **Thermal Coefficients as a Function of Pressure**

The thermal resistance and thermal capacitance are known at two pressures, 100.3 kPa and an average low pressure of 996.6 Pa. In order to establish a dependence of the thermal parameters on pressure, a linear regression is utilized. The thermal resistance as a function of pressure is approximated by

$$R_P = 4.129 \times 10^{-6} P + 4.3883 \ (K/W) \tag{6}$$

and the thermal capacitance is

$$C_P = -0.00736 P + 1348.514 \ (J/K). \tag{7}$$

These curves are depicted in Fig. 5.

It is known that the thermal conductivity of many materials, including foams, decreases with a decrease in pressure [12]. Thus, the conductive thermal resistance of such materials increases with decreasing pressure which is an intuitive result as a foam becomes more like a vacuum in which no conduction takes place. Therefore, it is interesting to note that the thermal resistance of the gondola decreases with a decreasing pressure.
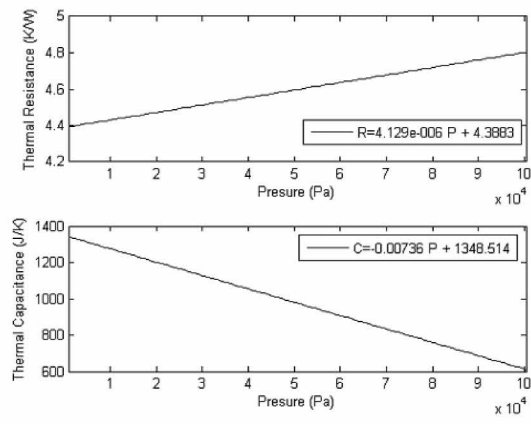
Fig. 5 Thermal coefficient pressure dependence.

- **Identification of Launch-Altitude Solar Input**

In order to obtain the solar input, Q_{sun}, at the launch altitude, the internal heat source, Q_H, was zeroed and the gondola was placed in direct sunlight and the payload was allowed to reach a near steady-state temperature. A thermocouple was utilized to measure the payload temperature on one minute intervals. A plot of the collected data is depicted in Fig. 6. The average outside atmospheric temperature was also measured in a shaded area with sufficient convection to be 298.2 K.

Again, a nonlinear weighted least-squares algorithm was used to fit a curve in the form of (3) to the collected data. Although it is not of direct use for this task, the identified time constant was found to be $R_P C_P = 3095.5$. This value is reassuringly close to the time-constant identified when the payload was heated internally, thus lending
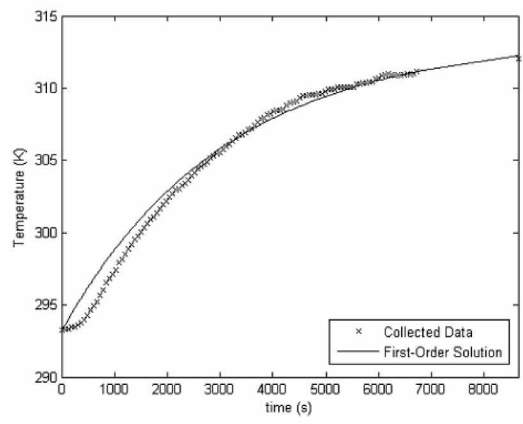
Fig. 6 Solar input experiment.

support to the validity of the structure of the model. Of more importance to the search for Q_{sun} is the the identified steady-state temperature, $T(\infty){=}313.5\ (K)$. Utilizing the previously identified thermal resistance, $R_P{=}4.8025\ (K/W)$, the following relation provides an expression for calculating the solar input

$$Q_{sun}{=}\frac{T(\infty){-}T_{out}}{R_P}.$$ (8)

This method yields $Q_{sun}{=}3.1889\ (W)$.

IV.   Thermal Controller

The feedback thermal controller heating elements are sized assuming worst-case conditions. This implies $Q_{sun}{=}0\ (W)$ and the minimum value for T_{out}. In this situation Eq. (6) can be rearranged into

$$Q_H{=}\frac{T(\infty){-}T_{out}}{R_P}\ .$$ (9)

Here, the steady-state temperature, $T(\infty)$, is a design parameter and is selected as the desired minimum steady-state payload temperature. The computation of (9) provides the amount of heat in Watts that must be applied to the system in a worst-case situation in order to maintain the steady-state payload temperature at a desired value. Utilizing a minimum payload temperature of 292 K and a minimum outside temperature of 250 K, the required heat is 8.7 W. In order to achieve this value a resistive heat source comprised of six $15\ \Omega$ resistors powered from a 4.5 V supply is utilized. This configuration ideally dissipates 8.1 W, which was determined to be acceptably close to the required heat input.

To ensure that the internal heat source does not generate excessive heat, which may lead to damage of the payload, a bang-off feedback controller is utilized. A schematic of the controller is depicted in Fig. 7. A TLV2454 operational amplifier is configured as a comparator with two inputs; one input is from a potentiometer which is utilized to create a setpoint below which the heaters are to turn-on. The other comparator input is connected to a temperature sensing network. As the NTC thermistor heats up, its resistance decreases which leads to a decrease in the voltage on the positive operational amplifier input. When this voltage drops below the voltage seen on the negative operational amplifier input, the operational amplifier's output saturates at the ground rail and turns off the MOSFET which, in turn, stops the current flow through the resistive heaters. When the NTC thermistor cools off, its resistance increases and so does the voltage on the positive operational amplifier input. When this voltage rises
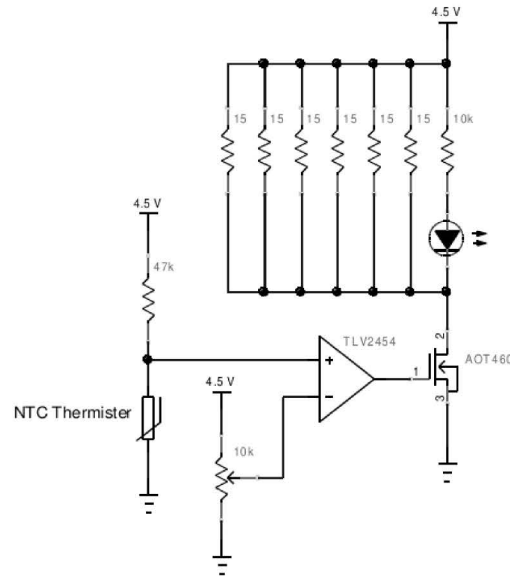
Fig. 7 Bang-off temperature controller.

above the setpoint voltage on the negative input, the operational amplifier's output saturates at the 4.5 V rail and turns on the MOSFET which then allows current to flow through the heaters. In future implementations, the operational amplifier should be replaced with a dedicated comparator.

In order to assist in adjusting the setpoint, a light emitting diode is utilized to indicate when the heaters are on. The setpoint for the flight was adjusted so that the heaters turn on when the payload temperature drops below room temperature, 294 K. Through the use of the controller, the heat supplied by the resistive heaters becomes a function of the payload temperature:

$$Q_H(T_P) = \begin{cases} 8.1 & for\ T_P < 294 \\ 0 & for\ T_P \geq 294 \end{cases}. \tag{10}$$

V. Flight Results

The validity of both the closed-loop pressure-independent model,

$$610.18\frac{dT_p}{dt} = -\frac{1}{4.8025}\left(T_p - T_{out}\right) + Q_H(T_P) + 3.1889, \tag{11}$$

and the closed-loop pressure-dependent model,

$$C_P(P)\frac{dT_P}{dt} = -\frac{1}{R_P(P)}\left(T_p - T_{out}\right) + Q_H(T_P) + 3.1889 \; , \tag{12}$$

is tested with flight data recorded by the payload pictured in Fig. 1. The measured data includes the internal payload temperature, the ambient outside atmosphere temperature, and the atmospheric pressure. In order to carry out the validation tests, Eq. (11) and Eq. (12) are integrated with respect to time utilizing the measured T_{out} and the computed feedback from (10) as inputs. Due to the varying conditions that occurred before launch, which involved the final assembly and handling of the payload, an initial-condition for the integration was selected at $t=2200 \; (s)$ which corresponds to approximately the moment of launch as indicated by the measured pressure and GPS-recorded altitude depicted in Fig. 8. The payload temperature predicted by the pressure-independent model and pressure-dependent model are plotted in Fig. 8 and Fig. 9, respectively.

Both models provide relatively good predictions of the payload temperature. The maximum error in temperature in each case is less than 6.8 K and this occurs during the last 10 km of the descent. It is very likely that this error is caused by neglecting the forced-air convection from the model. This seems especially likely considering the high-rate of descent, which is nearly double that of the ascent, through the thick and cold atmosphere that is encountered between 8000 and 9000 seconds. Although less pronounced, both models also predict slightly warmer temperatures between 4000 and 6000 seconds. The atmosphere is thinner in this region, according to Fig. 8, so the effects of the un-modeled forced-air convection are not as significant. The only region where the predicted temperature is noticeably less than the measured temperature occurs at around 7000 seconds which corresponds to the apex of the flight. This anomaly, though small, is probably related to the fact that the
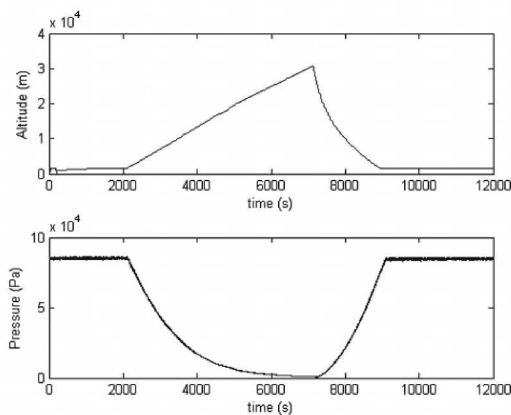
Fig. 8 Measured altitude and pressure.
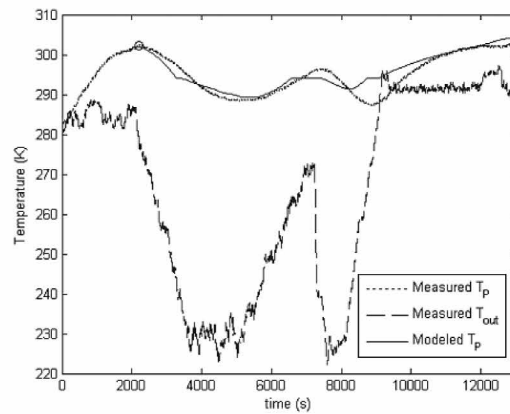
Fig. 9 Pressure-independent model response.

radiative heat-transfer effects are not thoroughly modeled. Still, the error in the predicted temperature for both models is less than 3 K at that altitude.

The control system's effects are clearly visible in the predicted responses in Figs. 9 and 10 as evident by the sudden changes induced by the instantaneous application of heat. However, the effects are not visible in the measured response. This is expected. Since the resistive heaters must undergo a thermal transient, there is substantial low-pass filtering of the step-like input applied by the controller which results in a smooth payload temperature evolution.

VI.   Conclusion

For short-duration flights in which a high-altitude float is not sustained, there does not appear to be a substantial
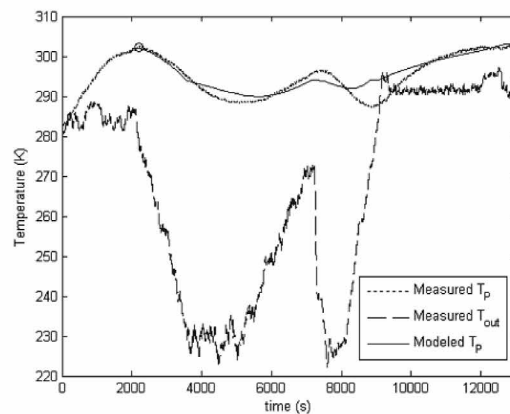
Fig. 10 Pressure-dependent model response.

benefit to adopting a pressure-dependent thermal model. However, the identification procedure and validation should be carried out on several different payloads to decrease the possibility that the results presented in this paper are specific to the one gondola for which the procedure was administered. The implications of adopting a pressure-independent modeling scheme would be beneficial since the system identification experiments can be easily carried out with a minimal amount of equipment.

Future research in the area of active temperature control should examine methods of quantifying the effectiveness of the control systems. This may involve flying two identical gondolas in which the control system has been deactivated in one of them. Another interesting topic, assuming that a valid model can be identified, would be to study the controller as a fuel-optimal problem especially since such an approach typically results in a bang-bang or bang-off structure.

Acknowledgments

References

[1] Hazen, N.L., "Assuring Payload Security in Flight and Recovery: Design Approaches and Flight Experience", *Advances in Space Research*, Vol. 5, No. 1, 1985, pp. 57-60

[2] Lichfield, E.W., Carlson, N.E., "Temperature Control of Balloon Packages", NCAR Technical Notes, NCAR-TN-32, 1967

[3] Kreith, F., Warren, J., "Thermal Analysis of Balloon-Borne Instrument Packages", NCAR Technical Notes, NCAR-TN-45, 1970.

[4] Carlson, L.A., "Thermal Analysis Program", *Atmospheric Technology*, No. 5, 1974, pp. 40-43

[5] Carlson, L.A., Brandeberry, P.M., "Thermal Analysis of Long Duration Flight Packages", *Proceedings: 8th AFCRL Scientific Balloon Symposium*, 1974, pp. 163-173

[6] Minichiello, A., "COTS in Space: Developing an Environmental Control System for Balloon-Borne Air-Cooled Electronics", *Proceedings: Tenth Intersociety Conference on Thermal and Thermomechanical Phenomena in Electronics Systems*, 2006, pp.1390-1399

[7] Spencer, S., Clark, D., Parnell, T.A., "The Design and Analysis of the Thermal Control System for the JACEE High Altitude Long Duration Balloon Flight, *Advanced Space Research*, Vol. 17, No. 9, 1996, pp. 91-94

[8] Fortescue, P., Swinerd, G., Stark, J., *Spacecraft Systems Engineering*, 4th Edition, John Wiley and Sons, West Sussex, UK, 2011

[9] Shearer, J.L., Kulakowski, B.T., Gardner J.F., *Dynamic Modeling and Control of Engineering Systems*, Prentice Hall, Upper Saddle River, NJ, 1996

[10] Özisik, M.N., *Heat Transfer*, McGraw-Hill Publishing Company, New York, 1985

[11] Norton, J.P., *An Introduction to System Identification*, Dover Publications, Mineola, NY, 1986

[12] Wu, J-W., Sung, W-F., Chu, H-S., "Thermal Conductivity of Polyurethane Foams", *International Journal of Heat and Mass Transfer*, No. 42, 1999, pp. 2211-2217